

Supporting Information for

**Topology-Guided Design of the 3D Penta-COFs
with Superior Ultraviolet Optical Response**

Xinyuan Ma ^a, Peng-Hu Du ^a, Changsheng Hou ^a, Chenxin Zhang ^a, Wei Sun ^a, Qing Zhang ^{a*},
and Qian Wang ^{a*}

^a *School of Materials Science and Engineering, Peking University, Beijing 100871, China*

* E-mail: q_zhang@pku.edu.cn; qianwang2@pku.edu.cn.

Note S1. Geometric feasibility analysis of four topologies (ung**, **unn**, **unh**, **unj**).**

As shown in **Table S1**, all of the topologies in this table are four-coordinate. Due to the bonding preference of 3D COFs, four-coordinate nodes typically form a 3D network in a tetrahedral arrangement with an ideal bond angle of $\theta_0 = 109.471^\circ$. Although COFs generally exhibit some tolerance for structural distortion, it is undesirable to deviate too much from ideal geometric features as they may lead to structural deformation or collapse.^{1,2} To quantify this geometric suitability, we introduce the bond angle average deviation $\nabla\bar{\theta}$ (

$$\nabla\bar{\theta} = \frac{\sum_i |\theta_i - \theta_0|}{N} \times 100\%, \text{ where } N \text{ is the number of four-coordinate bond angles}.$$

In addition, the edge length ratio ($|m|/|n|$) compares the difference of two types edges in the topology. A larger edge length difference implies greater difficulty in forming an ordered 3D framework. The results presented in this table indicate that among the four topologies, **unj** exhibits the smallest $\nabla\bar{\theta}$ and edge length ratio. In contrast, the other three topologies (**ung**, **unn**, and **unh**) show larger $\nabla\bar{\theta}$ (more than 25%) and edge ratios, making them less feasible for constructing stable 3D penta-COFs. Consequently, **unj** is selected as the target topology for further exploration.

Table S1. Structural parameters of the four topologies: including space group, bond angle average deviation $\nabla\bar{\theta}$ and edge length ratio $|m|/|n|$ for **unj**, **unh**, **ung** and **unn**.

| Topology | Space group | $\nabla\bar{\theta}$ (%) | ($ m / n $) |
|------------|--------------------------------------|--------------------------|---------------|
| ung | <i>R</i> -3c (No. 167) | 25.77 | 1.22 |
| unn | <i>R</i> -3c (No. 167) | 27.61 | 1.26 |
| unh | <i>P</i> 6 ₁ 22 (No. 178) | 29.29 | 1.32 |
| unj | <i>P</i> 6 ₁ 22 (No. 178) | 19.25 | 1.12 |

Note S2. Intrinsic chirality in the unj topology.

As shown in **Figure S1**, the **unj** topology intrinsically exhibits chirality, which can be classified into left-handed (*L*-) and right-handed (*R*-) structures due to the symmetry differences in the helical channels. The *L*-structure exhibits a counterclockwise helical arrangement, while the *R*-structure exhibits a clockwise helical arrangement. Despite this distinction, most properties of the *L*- and *R*-structures are identical, as the difference lies solely in the helical direction of the channels. Therefore, this study focuses on the *L*-structure as the representative for exploration in this study.

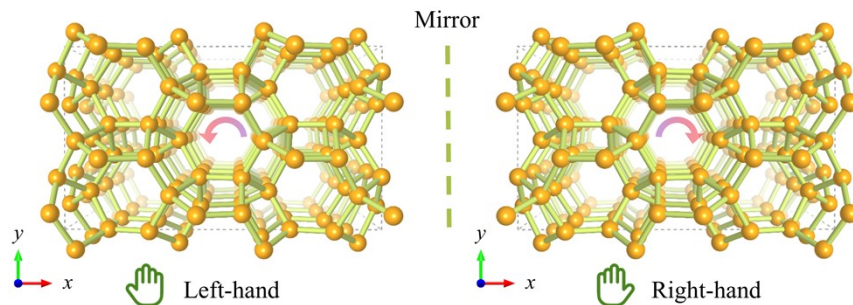


Fig. S1 Schematic illustration of the intrinsic chirality in the unj topology.

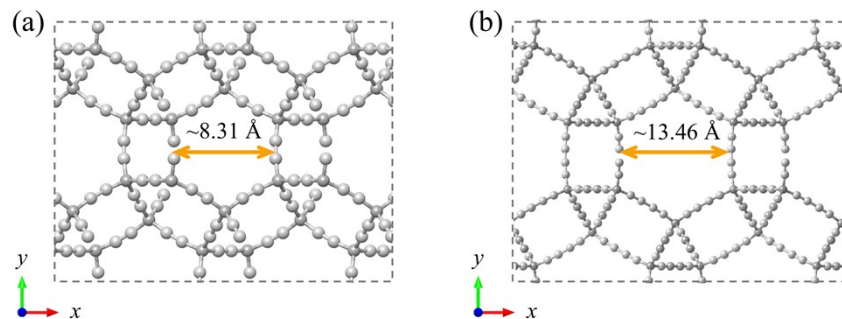


Fig. S2 Top views of unj-1 and unj-2, respectively.

Table S2. Structural parameters of the optimized unj-1 and unj-2: including lattice constants, primitive cell volume V_{cell} , bond angle average deviation $\nabla\bar{\theta}$, edge length ratio ($|\mathbf{m}|/|\mathbf{n}|$) and Wyckoff atiomic positions.

| Structure | Lattice constants (\AA) | V_{cell} (\AA^3) | $\nabla \bar{\theta}$ (%) | $ \mathbf{m} / \mathbf{n} $ | Wyckoff Atomic Positions |
|---------------|------------------------------------|--------------------------------------|---------------------------|-----------------------------|--------------------------------|
| unj -1 | $a = 9.54$ $c = 9.17$ | 722.07 | 1.05 | 1.01 | $12c$ (0.631, 0.699, 0.858) |
| | | | | | $12c$ (0.341, 0.572, 1.131) |
| | | | | | $6b$ (0.766, 0.234, 1.083) |
| unj -2 | $a = 15.44$ $c = 14.84$ | 3062.88 | 0.62 | 1.02 | $12c$ (0.594, 0.726, 0.881) |
| | | | | | $12c$ (0.639, 0.686, 0.850) |
| | | | | | $12c$ (0.768, 0.468, 0.823) |
| | | | 0.62 | 1.02 | $12c$ (0.768, 0.414, 0.883) |
| | | | | | $6b$ (0.766, 0.234, 1.083) |

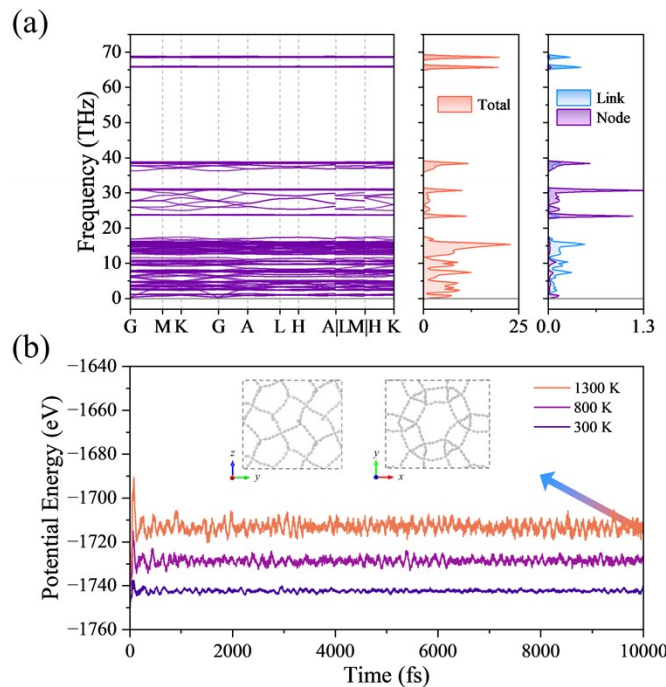


Fig. S3 Dynamical and thermal stability of unj-2: (a) phonon spectrum and phonon DOS. (b) AIMD simulations at 300, 800, and 1300 K, with insets showing the crystal structure snapshots in the end of the simulation at 1300 K.

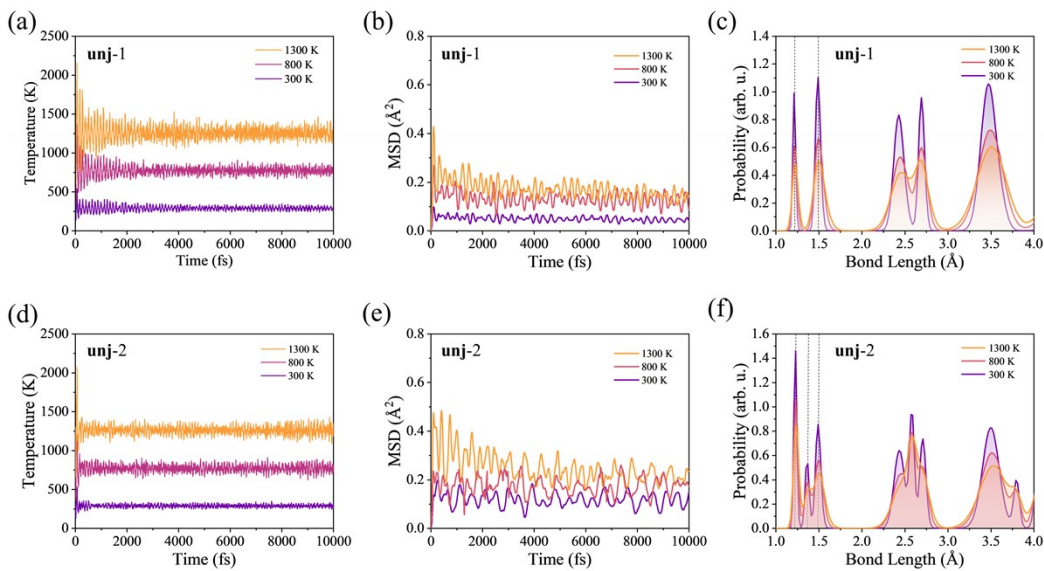


Fig. S4 AIMD simulations of unj-1 (a–c) and unj-2 (d–f) at 300, 800, and 1300 K: (a, d) temperature evolution, (b, e) mean square displacements (MSD), and (c, f) bond length distributions. The black dashed lines indicate the characteristic bond lengths in each structure.

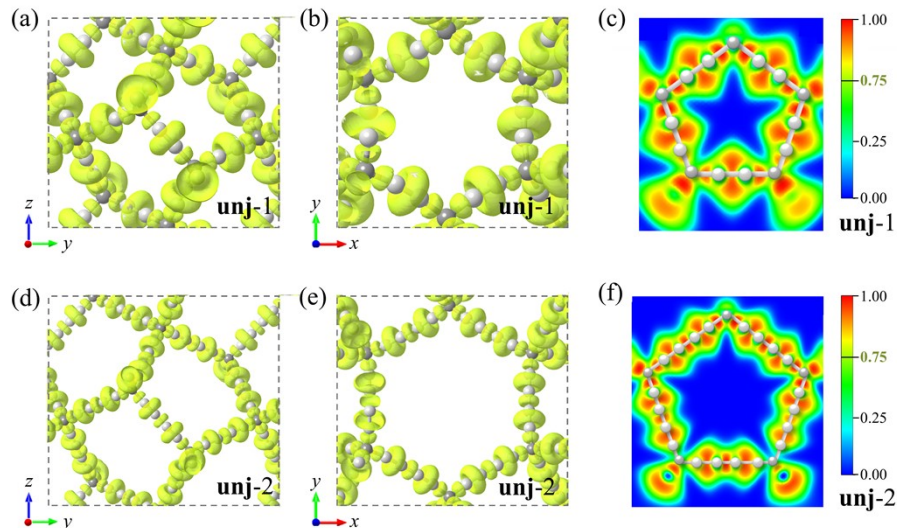


Fig. S5 ELF distribution of unj-1 and unj-2: (a, d) perspective views (isovalue = 0.75 \AA^{-3}), (b, e) top views (isovalue = 0.75 \AA^{-3}), (c, f) sectional views along the pentagonal ring.

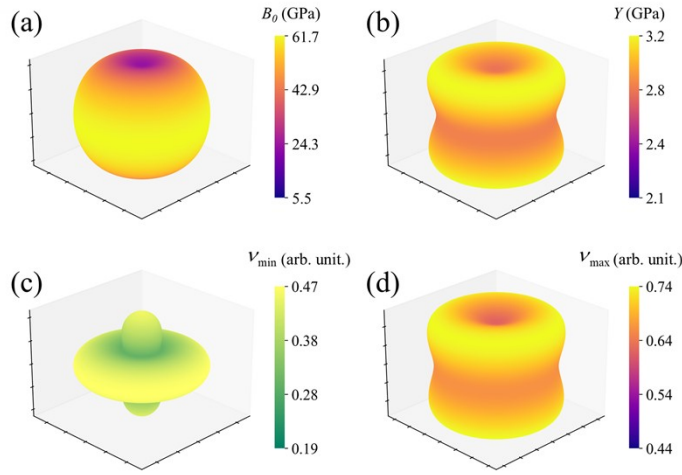
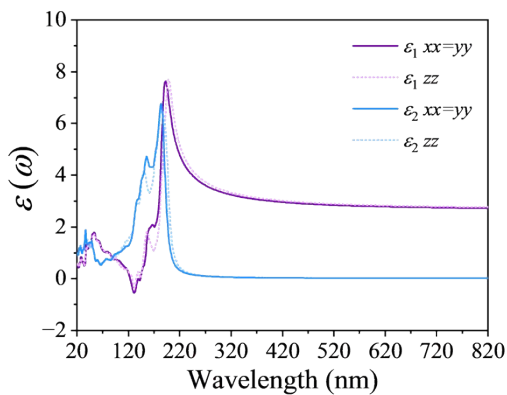


Fig. S6 3D Anisotropy mechanical properties of unj-2: (a) bulk modulus B_0 , (b) Young's modulus Y , and the (c) minimum and (d) maximum Poisson's ratios ν_{\min} , ν_{\max} .

Table S3. Statistical summary of mechanical properties: including the topology, coordination number (CN) and ratio, density, bulk modulus B_0 and the Poisson's ratio ν . For comparability, reference materials containing at most a single alkyne bond between two carbon nodes were selected.

| No. | Material | Topology | CN (ratio) | Density (g/cm ³) | B_0 (GPa) | ν (arb. unit.) |
|-----|--------------------------------|--------------|------------|------------------------------|-------------|--------------------|
| 1 | unj-1 | unj | 2,4 (4:1) | 0.82 | 73.69 | 0.44 |
| 2 | Cubic a-Graphyne ³ | pbz | 2,3 (1:1) | 1.04 | 99.80 | 0.42 |
| 3 | Cubic b-Graphyne ³ | pbz | 2,3 (1:1) | 1.44 | 150.45 | 0.45 |
| 4 | Rh12 ⁴ | pcu-h | 2,3 (1:1) | 1.77 | 108.60 | 0.34 |
| 5 | Cubic Graphiteyne ³ | pbz | 2,3 (2:1) | 1.04 | 110.82 | 0.31 |
| 6 | TY carbon ⁵ | dia-a | 2,4 (1:1) | 0.83 | 84.51 | 0.44 |
| 7 | supercubane C32 ⁶ | pcb | 2,4 (1:1) | 1.33 | 135.71 | 0.35 |
| 8 | Y-II carbon ⁷ | dia | 2,4 (1:1) | 1.78 | 167.51 | 0.43 |
| 9 | 1-Yne ⁸ | crb | 2,4 (2:1) | 1.911 | 160.00 | 0.35 |

| | | | | | | |
|----|-----------------------------|--------------|-----------|-------|--------|------|
| 10 | 2-Yne ⁸ | crb | 2,4 (2:1) | 1.650 | 114.80 | 0.33 |
| 11 | Y-carbon ⁵ | dia | 2,4 (4:1) | 0.90 | 84.40 | 0.47 |
| 12 | 6.82 P ⁹ | pbp | 3 | 2.01 | 226.09 | 0.38 |
| 13 | Cubic Graphite ⁹ | pbz | 3 | 2.14 | 248.25 | 0.29 |
| 14 | Squareglitter ¹⁰ | mjb | 3,4 (1:1) | 2.35 | 275.01 | 0.30 |
| 15 | bcc-C20 ¹¹ | tfh | 3,4 (1:1) | 2.42 | 203.84 | 0.20 |
| 16 | T6 ¹² | tfi | 3,4 (1:1) | 2.95 | 326.71 | 0.29 |
| 17 | 3D-(4,0) ¹³ | xca | 3,4 (1:2) | 3.24 | 368.88 | 0.13 |
| 18 | Diamond | dia | 4 | 3.50 | 432.90 | 0.07 |
| 19 | T-carbon ⁷ | dia | 4 | 1.50 | 169.00 | 0.33 |
| 20 | T12 ¹⁴ | cdp | 4 | 3.47 | 424.80 | 0.09 |
| 21 | L-carbon ¹² | lon-a | 4 | 1.52 | 162.40 | 0.37 |
| 22 | HP3 ¹⁵ | qtz | 4 | 3.69 | 447.06 | 0.06 |
| 23 | CA2 ¹⁶ | acs-a | 4 | 2.23 | 234.59 | 0.26 |
| 24 | C8 ¹⁷ | pcb | 4 | 2.79 | 311.00 | 0.22 |



Fig, S7 Frequency-dependent dielectric function of unj-1.

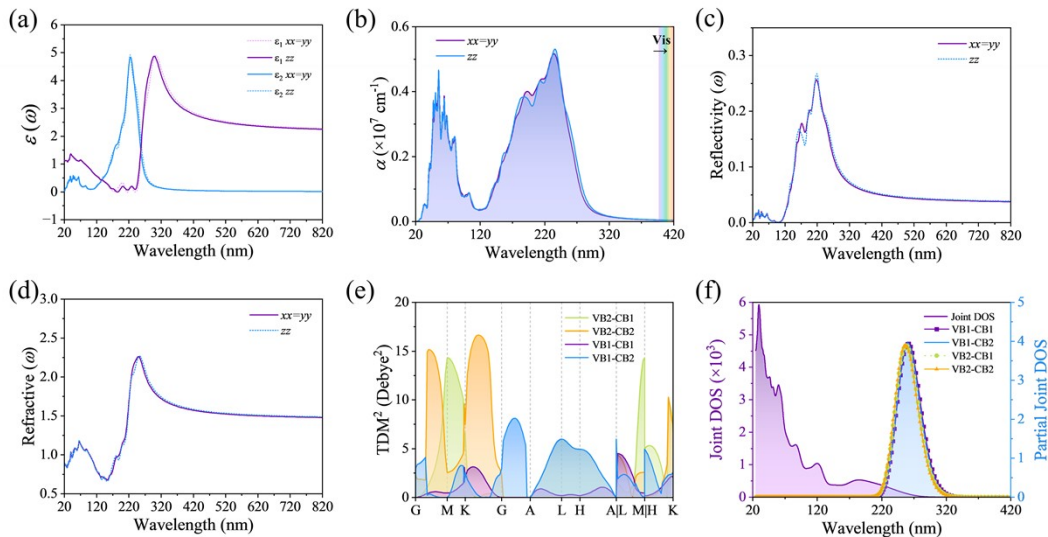


Fig. S8 Linear optical properties of unj-2: (a) frequency-dependent dielectric function, (b) absorption spectrum, (c) reflection spectrum, (d) refractive index spectrum. (e) Squared transition dipole moments, (f) joint DOS and partial joint DOS, where the VB1, VB2, CB1 and CB2 refer to the energy bands near the band edge.

Note S3. SHG susceptibilities $\chi_{ij}^{(2)}$ for **L-unj-1** and **R-unj-1**.

As shown in **Figure S9**, the crystal symmetry restricts the nonzero components of the $\chi_{ij}^{(2)}$, requiring $\chi_{14} = -\chi_{25}$ (where the subscripts denote the tensor components, with 1=x, 2=y, 4=yz=zy, 5=xz=zx). Consequently, the analysis focuses on the χ_{14} component. The maximum values of the real part of $\chi_{14}(\omega)$ are -1.03 pm/V for **L-unj-1** and 1.07 pm/V for **R-unj-1**, both located at 3.34 eV. For imaginary part, the corresponding maxima are 0.80 pm/V for **L-unj-1** and -1.28 pm/V for **R-unj-1**, both occur at 3.28 eV. These values exhibit comparable magnitudes but opposite signs, consistent with their opposite chirality.

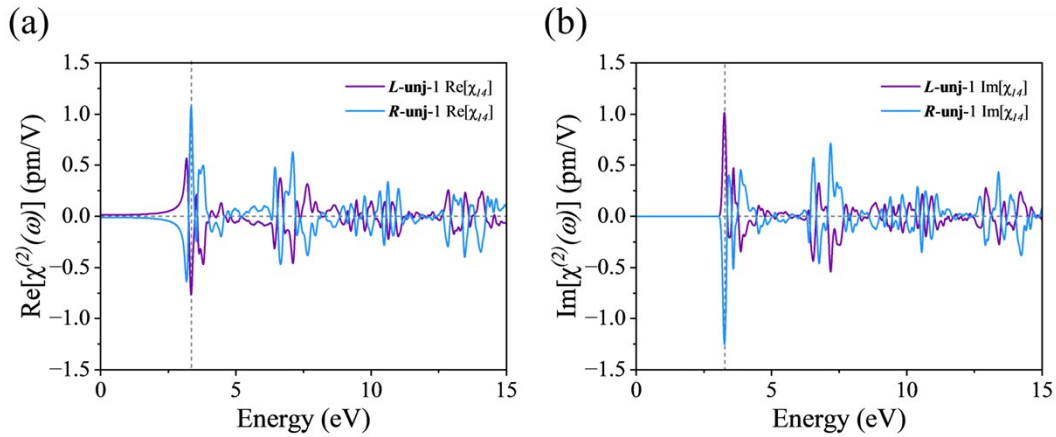


Fig. S9 Real part and imaginary part of the SHG susceptibilities $\chi_{ij}^{(2)}$ for *L-unj-1* and *R-unj-1*.

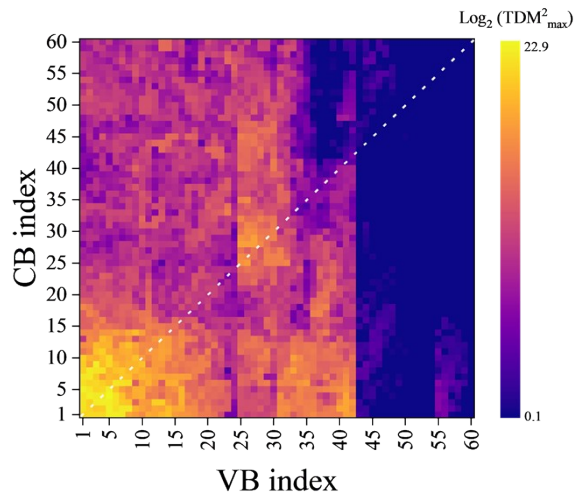


Fig. S10 Squared transition dipole moments (TDM²) between 60 valence bands and 60 conduction bands of unj-1. The white dashed line is included for visual guidance along the band-index diagonal.

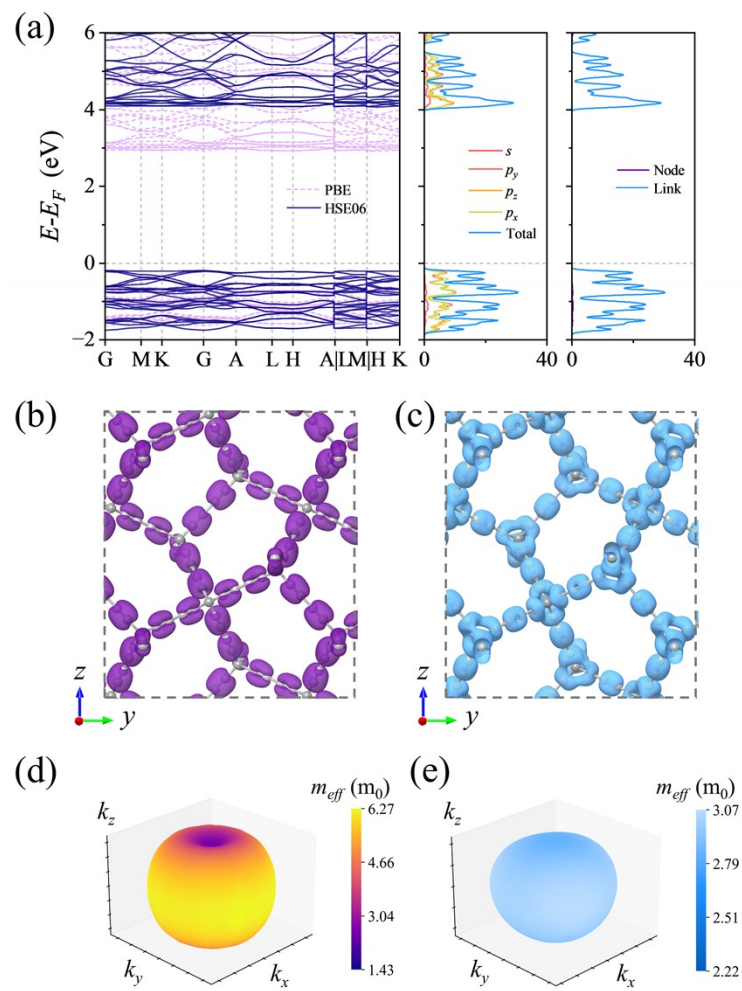


Fig. S11 Electronic properties of unj-2: (a) band structure with the bandgap of 4.28 eV and partial DOS at the HSE06 level, (b, c) band-partial charge distributions at the VBM and CBM (isovalue = 0.0008 Å⁻³). (d, e) 3D anisotropic effective mass (m_{eff}) at the VBM (absolute values for better visualization) and the CBM.

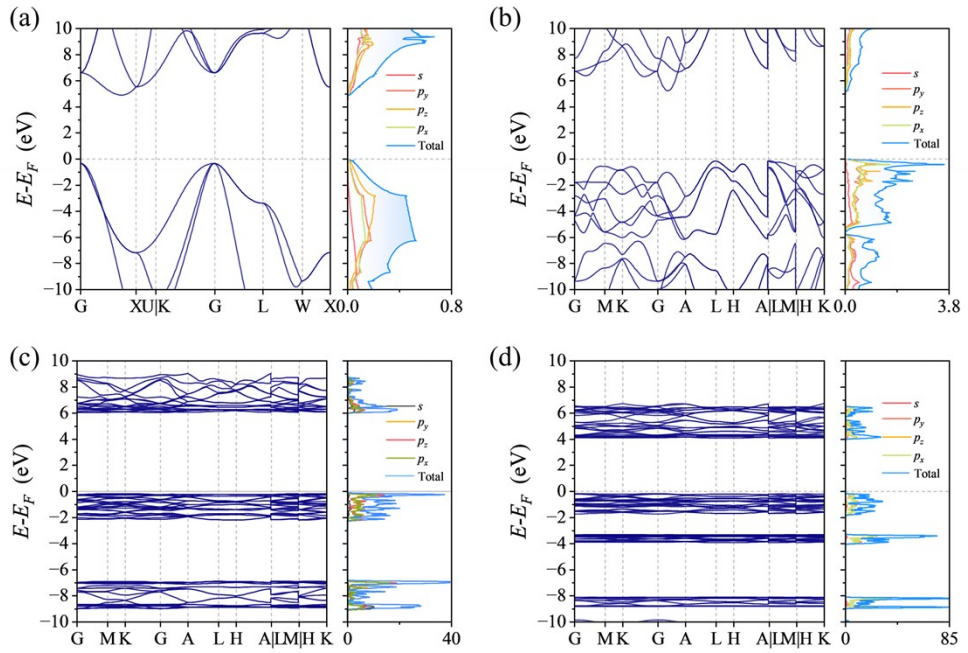


Fig. S12 Band structures and DOS at the HSE06 level: (a) **dia**, (b) **unj**, (c) **unj-1**, and (d) **unj-2**.

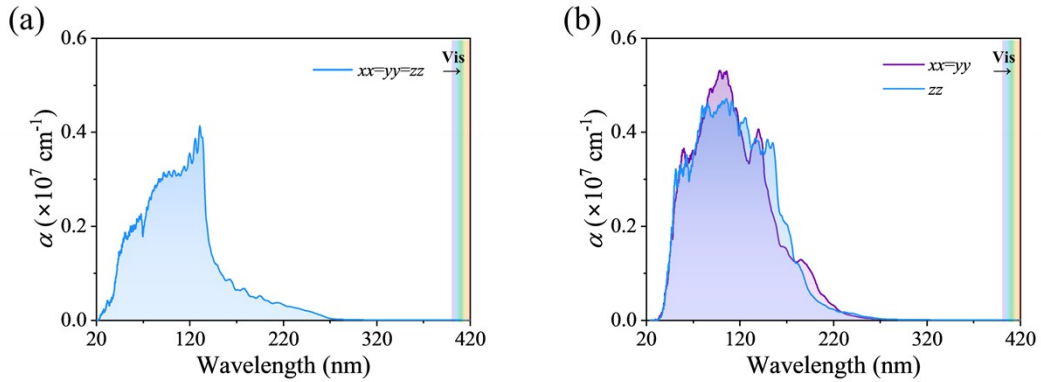


Fig. S13 Absorption spectra of (a) dia and (b) unj.

Appendix: POSCAR files of the main structures.

dia

| | | |
|--------------|--------------|---------------|
| 1.00000000 | | |
| 2.5253059067 | 0.0000000000 | 0.0000000000 |
| 1.2626529533 | 2.1869790675 | -0.0000000000 |
| 1.2626529533 | 0.7289930225 | 2.0619036386 |

C

2

Direct

| | | |
|---------------|---------------|--------------|
| 0.2500000000 | 0.2500000000 | 0.2500000000 |
| -0.0000000000 | -0.0000000000 | 0.0000000000 |

unj

1.0

| | | |
|---------------|--------------|--------------|
| 3.5734000206 | 0.0000000000 | 0.0000000000 |
| -1.7867000103 | 3.0946551957 | 0.0000000000 |
| 0.0000000000 | 0.0000000000 | 3.3787999153 |

C

6

Direct

| | | |
|-------------|-------------|-------------|
| 0.767430000 | 0.232570000 | 0.916666687 |
| 0.767430000 | 0.534860000 | 0.250000020 |
| 0.465140000 | 0.232570000 | 0.583333353 |
| 0.232570000 | 0.767430000 | 0.416666687 |
| 0.232570000 | 0.465140000 | 0.750000020 |
| 0.534860000 | 0.767430000 | 0.083333353 |

unj-1

1.0

| | | |
|---------------|--------------|--------------|
| 9.5366001129 | 0.0000000000 | 0.0000000000 |
| -4.7683000565 | 8.2589379635 | 0.0000000000 |
| 0.0000000000 | 0.0000000000 | 9.1676998138 |

C

30

Direct

| | | |
|-------------|-------------|-------------|
| 0.631140000 | 0.698850000 | 0.858370000 |
| 0.301150000 | 0.932290000 | 0.525036667 |

| | | |
|-------------|-------------|-------------|
| 0.067710000 | 0.368860000 | 0.191703333 |
| 0.368860000 | 0.301150000 | 0.358370000 |
| 0.698850000 | 0.067710000 | 0.025036667 |
| 0.932290000 | 0.631140000 | 0.691703333 |
| 0.698850000 | 0.631140000 | 0.808296667 |
| 0.932290000 | 0.301150000 | 0.141630000 |
| 0.368860000 | 0.067710000 | 0.474963333 |
| 0.301150000 | 0.368860000 | 0.308296667 |
| 0.067710000 | 0.698850000 | 0.641630000 |
| 0.631140000 | 0.932290000 | 0.974963333 |
| 0.340870000 | 0.572400000 | 0.131430000 |
| 0.427600000 | 0.768470000 | 0.798096667 |
| 0.231530000 | 0.659130000 | 0.464763333 |
| 0.659130000 | 0.427600000 | 0.631430000 |
| 0.572400000 | 0.231530000 | 0.298096667 |
| 0.768470000 | 0.340870000 | 0.964763333 |
| 0.572400000 | 0.340870000 | 0.535236667 |
| 0.768470000 | 0.427600000 | 0.868570000 |
| 0.659130000 | 0.231530000 | 0.201903333 |
| 0.427600000 | 0.659130000 | 0.035236667 |
| 0.231530000 | 0.572400000 | 0.368570000 |
| 0.340870000 | 0.768470000 | 0.701903333 |
| 0.766000000 | 0.234000000 | 0.083333336 |
| 0.766000000 | 0.532000000 | 0.750000002 |
| 0.468000000 | 0.234000000 | 0.416666669 |
| 0.234000000 | 0.766000000 | 0.583333336 |
| 0.234000000 | 0.468000000 | 0.250000002 |
| 0.532000000 | 0.766000000 | 0.916666669 |

unj-2

1.0

| | | |
|---------------|---------------|---------------|
| 15.4399995804 | 0.0000000000 | 0.0000000000 |
| -7.7199997902 | 13.3714318710 | 0.0000000000 |
| 0.0000000000 | 0.0000000000 | 14.8355998993 |

C

54

Direct

| | | |
|-------------|-------------|-------------|
| 0.594100000 | 0.725660000 | 0.880990000 |
|-------------|-------------|-------------|

| | | |
|-------------|-------------|-------------|
| 0.274340000 | 0.868440000 | 0.547656667 |
| 0.131560000 | 0.405900000 | 0.214323333 |
| 0.405900000 | 0.274340000 | 0.380990000 |
| 0.725660000 | 0.131560000 | 0.047656667 |
| 0.868440000 | 0.594100000 | 0.714323333 |
| 0.725660000 | 0.594100000 | 0.785676667 |
| 0.868440000 | 0.274340000 | 0.119010000 |
| 0.405900000 | 0.131560000 | 0.452343333 |
| 0.274340000 | 0.405900000 | 0.285676667 |
| 0.131560000 | 0.725660000 | 0.619010000 |
| 0.594100000 | 0.868440000 | 0.952343333 |
| 0.639270000 | 0.686290000 | 0.850320000 |
| 0.313710000 | 0.952980000 | 0.516986667 |
| 0.047020000 | 0.360730000 | 0.183653333 |
| 0.360730000 | 0.313710000 | 0.350320000 |
| 0.686290000 | 0.047020000 | 0.016986667 |
| 0.952980000 | 0.639270000 | 0.683653333 |
| 0.686290000 | 0.639270000 | 0.816346667 |
| 0.952980000 | 0.313710000 | 0.149680000 |
| 0.360730000 | 0.047020000 | 0.483013333 |
| 0.313710000 | 0.360730000 | 0.316346667 |
| 0.047020000 | 0.686290000 | 0.649680000 |
| 0.639270000 | 0.952980000 | 0.983013333 |
| 0.767570000 | 0.467640000 | 0.823240000 |
| 0.532360000 | 0.299930000 | 0.489906667 |
| 0.700070000 | 0.232430000 | 0.156573333 |
| 0.232430000 | 0.532360000 | 0.323240000 |
| 0.467640000 | 0.700070000 | 0.989906667 |
| 0.299930000 | 0.767570000 | 0.656573333 |
| 0.467640000 | 0.767570000 | 0.843426667 |
| 0.299930000 | 0.532360000 | 0.176760000 |
| 0.232430000 | 0.700070000 | 0.510093333 |
| 0.532360000 | 0.232430000 | 0.343426667 |
| 0.700070000 | 0.467640000 | 0.676760000 |
| 0.767570000 | 0.299930000 | 0.010093333 |
| 0.768030000 | 0.413950000 | 0.883310000 |
| 0.586050000 | 0.354080000 | 0.549976667 |
| 0.645920000 | 0.231970000 | 0.216643333 |
| 0.231970000 | 0.586050000 | 0.383310000 |

| | | |
|-------------|-------------|-------------|
| 0.413950000 | 0.645920000 | 0.049976667 |
| 0.354080000 | 0.768030000 | 0.716643333 |
| 0.413950000 | 0.768030000 | 0.783356667 |
| 0.354080000 | 0.586050000 | 0.116690000 |
| 0.231970000 | 0.645920000 | 0.450023333 |
| 0.586050000 | 0.231970000 | 0.283356667 |
| 0.645920000 | 0.413950000 | 0.616690000 |
| 0.768030000 | 0.354080000 | 0.950023333 |
| 0.765920000 | 0.234080000 | 0.083333336 |
| 0.765920000 | 0.531840000 | 0.750000002 |
| 0.468160000 | 0.234080000 | 0.416666669 |
| 0.234080000 | 0.765920000 | 0.583333336 |
| 0.234080000 | 0.468160000 | 0.250000002 |
| 0.531840000 | 0.765920000 | 0.916666669 |

References

- (1) Yaghi, O. M.; Kalmutzki, M. J.; Diercks, C. S. *Introduction to Reticular Chemistry: Metal-Organic Frameworks and Covalent Organic Frameworks*, 1st ed.; Wiley, 2019. <https://doi.org/10.1002/9783527821099>.
- (2) Guo, Z.; Zhang, Z.; Sun, J. Topological Analysis and Structural Determination of 3D Covalent Organic Frameworks. *Adv. Mater.* **2024**, *36* (19), 2312889. <https://doi.org/10.1002/adma.202312889>.
- (3) Baughman, R. H.; Cui, C. Polymers with Conjugated Chains in Three Dimensions. *Synth. Met.* **1993**, *55* (1), 315–320. [https://doi.org/10.1016/0379-6779\(93\)90951-R](https://doi.org/10.1016/0379-6779(93)90951-R).
- (4) Wang, J.-T.; Chen, C.; Li, H.-D.; Mizuseki, H.; Kawazoe, Y. Three-Dimensional Carbon Allotropes Comprising Phenyl Rings and Acetylenic Chains in Sp⁺sp² Hybrid Networks. *Sci. Rep.* **2016**, *6* (1), 24665. <https://doi.org/10.1038/srep24665>.
- (5) Jo, J. Y.; Kim, B. G. Carbon Allotropes with Triple Bond Predicted by First-Principle Calculation: Triple Bond Modified Diamond and \$T\$-Carbon. *Phys. Rev. B* **2012**, *86* (7), 75151. <https://doi.org/10.1103/PhysRevB.86.075151>.
- (6) Srinivasu, K.; Ghosh, S. K. Electronic Structure, Optical Properties, and Hydrogen Adsorption Characteristics of Supercubane-Based Three-Dimensional Porous Carbon. *J. Phys. Chem. C* **2012**, *116* (47), 25015–25021. <https://doi.org/10.1021/jp3104479>.
- (7) Sheng, X.-L.; Yan, Q.-B.; Ye, F.; Zheng, Q.-R.; Su, G. T-Carbon: A Novel Carbon Allotrope. *Phys. Rev. Lett.* **2011**, *106* (15), 155703. <https://doi.org/10.1103/PhysRevLett.106.155703>.
- (8) Kim, B. G.; Sim, H.; Park, J. C4 Carbon Allotropes with Triple-Bonds Predicted by First-Principles Calculations. *Solid State Commun.* **2013**, *169*, 50–56. <https://doi.org/10.1016/j.ssc.2013.07.001>.
- (9) O'Keeffe, M.; Adams, G. B.; Sankey, O. F. Predicted New Low Energy Forms of Carbon. *Phys. Rev. Lett.* **1992**, *68* (15), 2325–2328. <https://doi.org/10.1103/PhysRevLett.68.2325>.
- (10) Prasad, D. L. V. K.; Gerovac, N. M.; Bucknum, M. J.; Hoffmann, R. Squaroglitter: A 3,4-Connected Carbon Net.

- J. Chem. Theory Comput.* **2013**, *9* (8), 3855–3859. <https://doi.org/10.1021/ct4004367>.
- (11) Hu, M.; Tian, F.; Zhao, Z.; Huang, Q.; Xu, B.; Wang, L.-M.; Wang, H.-T.; Tian, Y.; He, J. Exotic Cubic Carbon Allotropes. *J. Phys. Chem. C* **2012**, *116* (45), 24233–24238. <https://doi.org/10.1021/jp3064323>.
 - (12) Zhang, S.; Wang, Q.; Chen, X.; Jena, P. Stable Three-Dimensional Metallic Carbon with Interlocking Hexagons. *Proc. Natl. Acad. Sci.* **2013**, *110* (47), 18809–18813. <https://doi.org/10.1073/pnas.1311028110>.
 - (13) Ribeiro, F. J.; Tangney, P.; Louie, S. G.; Cohen, M. L. Structural and Electronic Properties of Carbon in Hybrid Diamond-Graphite Structures. *Phys. Rev. B* **2005**, *72* (21), 214109. <https://doi.org/10.1103/PhysRevB.72.214109>.
 - (14) Zhao, Z.; Tian, F.; Dong, X.; Li, Q.; Wang, Q.; Wang, H.; Zhong, X.; Xu, B.; Yu, D.; He, J.; Wang, H.-T.; Ma, Y.; Tian, Y. Tetragonal Allotrope of Group 14 Elements. *J. Am. Chem. Soc.* **2012**, *134* (30), 12362–12365. <https://doi.org/10.1021/ja304380p>.
 - (15) Zhu, Q.; Oganov, A. R.; Salvadó, M. A.; Pertíerra, P.; Lyakhov, A. O. Denser than Diamond: Ab Initio Search for Superdense Carbon Allotropes. *Phys. Rev. B* **2011**, *83* (19), 193410. <https://doi.org/10.1103/PhysRevB.83.193410>.
 - (16) Greshnyakov, V. A.; Belenkova, E. A. Structures of Diamond-like Phases. *J. Exp. Theor. Phys.* **2011**, *113* (1), 86–95. <https://doi.org/10.1134/S1063776111060173>.
 - (17) Johnston, R. L.; Hoffmann, R. Superdense Carbon, C8: Supercubane or Analog of .Gamma.-Silicon? *J. Am. Chem. Soc.* **1989**, *111* (3), 810–819. <https://doi.org/10.1021/ja00185a004>.